Responses of gaseous sulfuric acid and particulate sulfate to reduced SO2 concentration : A perspective from long-term measurements in Beijing

Li, Xiaoxiao

2020-06-15

Li , X , Zhao , B , Zhou , W , Shi , H , Yin , R , Cai , R , Yang , D , Dällenbach , K , Deng , C , Fu , Y , Qiao , X , Wang , L , Liu , Y , Yan , C , Kulmala , M , Zheng , J , Hao , J , Wang , S & Jiang , J 2020 , ' Responses of gaseous sulfuric acid and particulate sulfate to reduced SO2 concentration : A perspective from long-term measurements in Beijing ' , The Science of the Total Environment , vol. 721 , 137700 . https://doi.org/10.1016/j.scitotenv.2020.137700

http://hdl.handle.net/10138/341617
https://doi.org/10.1016/j.scitotenv.2020.137700

Responses of gaseous sulfuric acid and particulate sulfate to reduced SO_2 concentration: a perspective from long-term measurements in Beijing

Xiaoxiao Li[1, 2], Bin Zhao[3], Wei Zhou[1, 2], Hongrong Shi[4], Rujing Yin[1, 2], Runlong Cai[1, 2, 6], Dongsen Yang[5], Kaspar Dällenbach[6], Chenjuan Deng[1, 2], Yueyun Fu[1, 2], Xiaohui Qiao[1, 2], Lin Wang[7], Yongchun Liu[8], Chao Yan[6, 8], Markku Kulmala[6, 8], Jun Zheng[5], Jiming Hao[1, 2], Shuxiao Wang[1, 2], Jingkun Jiang[1, 2*]

Affiliations:

[1] State Key Joint Laboratory of Environment Simulation and Pollution Control, School of Environment, Tsinghua University, Beijing 100084, China

[2] State Environmental Protection Key Laboratory of Sources and Control of Air Pollution Complex, Beijing 100084, China

[3] Pacific Northwest National Laboratory, Richland, WA 99352, USA

[4] Key Laboratory of Middle Atmosphere and Global Environment Observation, Institute of Atmospheric Physics, Chinese Academy of Sciences, Beijing, China

[5] Collaborative Innovation Center of Atmospheric Environment and Equipment Technology, Nanjing University of Information Science & Technology, Nanjing 210044, China

[6] Institute for Atmospheric and Earth System Research/Physics, Faculty of Science, University of Helsinki, 00014 Helsinki, Finland

[7] Shanghai Key Laboratory of Atmospheric Particle Pollution and Prevention (LAP[3]), Department of Environmental Science& Engineering, Jiangwan Campus, Fudan University, Shanghai 200438, China

[8] Aerosol and Haze Laboratory, Beijing Advanced Innovation Center for Soft Matter Science and Engineering, Beijing

University of Chemical Technology, 100029 Beijing, China

*: *Correspondence to*: J. Jiang (jiangjk@tsinghua.edu.cn)

Abstract: SO_2 concentration decreased rapidly in recent years in China due to the implementation of strict control policies by the government. Particulate sulfate (pSO_4^{2-}) and gaseous H_2SO_4 (SA) are two major products of SO_2 and they play important roles in the haze formation and new particle formation (NPF), respectively. We examined the change in pSO_4^{2-} and SA concentrations in response to reduced SO_2 concentration using long-term measurement data in Beijing. Simulations from the Community Multiscale Air Quality model with a 2-D Volatility Basis Set (CMAQ/2D-VBS) were used for comparison. From 2013 to 2018, SO_2 concentration in Beijing decreased by ~81% (from 9.1 ppb to 1.7 ppb). pSO_4^{2-} concentration in submicrometer particles decreased by ~60% from 2012-2013 (monthly average of ~10 $\mu g \cdot m^{-3}$) to 2018-2019 (monthly average of ~4 $\mu g \cdot m^{-3}$). Accordingly, the fraction of pSO_4^{2-} in these particles decreased from 20-30% to less than 10%. Increased sulfur oxidation ratio was observed both in the measurements and the CMAQ/2D-VBS simulations. Despite the reduction in SO_2 concentration, there was no obvious decrease in SA concentration based on data from several measuring periods from 2008 to 2019. This was supported by the increased SA:SO_2 ratio with reduced SO_2 concentration and condensation sink. NPF frequency in Beijing between 2004 and 2019 remains relatively constant. This constant NPF frequency is consistent with the relatively stable SA concentration in Beijing, while different from some other cities where NPF frequency was reported to decrease with decreased SO_2 concentrations.

Key words: sulfur dioxide, gaseous sulfuric acid, particulate sulfate, long-term observation, new particle formation

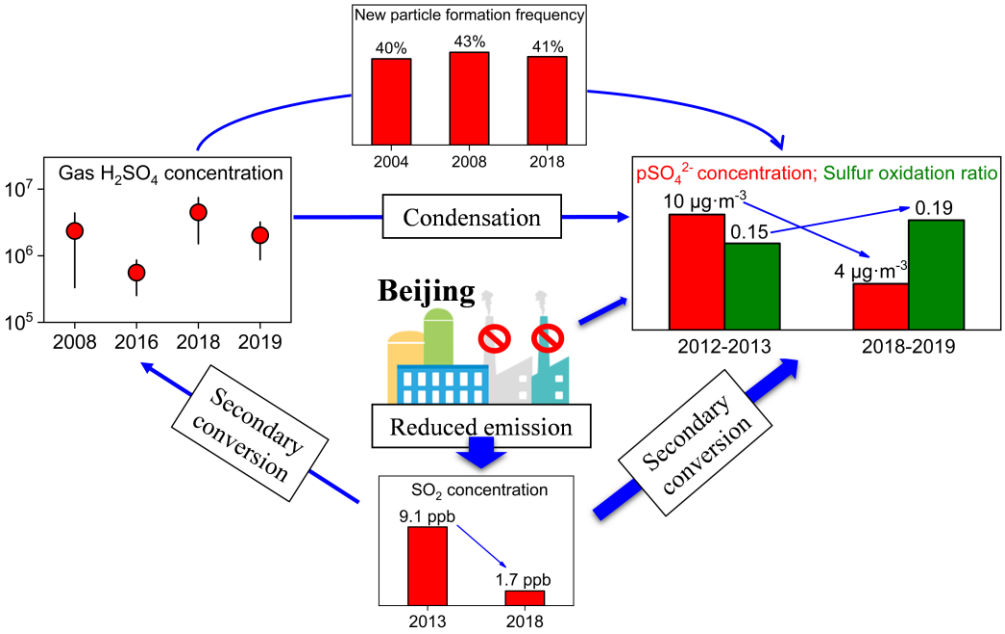

Highlights

- Particulate sulfate concentration and its fraction in submicrometer particles decreased from 2012 to 2019 in Beijing.
- Sulfur oxidation ratio increased from 2013 to 2019 in Beijing.
- Sulfuric acid concentration remains relatively stable based on several measuring periods from 2008 to 2019.
- The frequency of new particle formation events in Beijing remains relatively stable from 2004 to 2019.

1 INTRODUCTION

In Chinese megacities, both atmospheric new particle formation (NPF) and haze formation happen frequently (Chu et al., 2019; Guo et al., 2014; Zheng et al., 2016). Gaseous H_2SO_4 (SA) is the key precursor initiating NPF while particulate sulfate (pSO_4^{2-}) is one of the most important drivers for haze formation. Both of them are ubiquitous atmospheric sulfur-containing compounds that originate from the oxidation of SO_2 (Seinfeld and Pandis, 2006; Zhang et al., 2015). In recent decades, the anthropogenic emission of SO_2 has been reduced dramatically in China because of the implementation of strict control policies, and atmospheric SO_2 concentration was significantly reduced consequently

(Cheng et al., 2019; Wang et al., 2017; Xia et al., 2016; Zeng et al., 2019; Zhai et al., 2019). The formation of pSO_4^{2-} and SA may change in response to the SO_2 reduction. In megacities like Beijing and Shanghai, the oxidants for the formation of pSO_4^{2-} and SA are of high complexity (Cheng et al., 2016; Wang et al., 2016), and various non-linear processes may happen in such complex atmospheric environments (Wang et al., 2011a; Zhao et al., 2017).

Atmospheric SA is mainly produced from gas-phase oxidation of SO_2 by OH radicals (Finlayson-Pitts and Pitts, 1999; Kuang et al., 2008; Weber et al., 1999; Zhang et al., 2012). Thus, a decrease in SO_2 might lead to a decreasing production rate of SA, in the condition of no significant changes in the atmospheric oxidants. However, the condensational loss rate of SA to the particle surface may also decrease due to the reduced aerosol loading. Accurate measurement of atmospheric SA concentration is challenging because of its low concentration (10^5-10^8 #·cm^{-3}), short lifetime (less than 1 min), and the sticky nature (completely non-volatile) (Eisele and Tanner, 1993; Zhang et al., 2012; Zheng et al., 2011). Limited long-term measurements of SA were achieved until recently (Bertram et al., 2011; Birmili et al., 2003; Jokinen et al., 2012; Mikkonen et al., 2011). Several proxies were proposed to estimate atmospheric SA concentration (Dada et al., 2017; Lu et al., 2019; Mikkonen et al., 2011; Petaja et al., 2009), but the applicability of these proxies in different places and conditions remains to be tested.

A direct influence of changing SA concentration would be on atmospheric NPF. The occurrence of NPF was reported to decrease with reduced SO_2 concentration in a number of sites (Birmili and Wiedensohler, 2000; Hamed et al., 2010; Jaatinen et al., 2009; Kyro et al., 2014; Saha et al., 2018). The influences of reduced SO_2 concentration on NPF frequency were argued to be caused by a reduction in SA concentration. It was estimated in the model that if anthropogenic SO_2 emission is removed, particle formation potential from SA would drop by about two orders of magnitude (Perraud et al., 2015). However, due to the lack of direct SA measurements, it remains uncertain whether the observed reduction in NPF frequency in these sites is indeed attributed to reduced SA concentration. What's more, the

occurrence of NPF is also influenced by other factors. For instance, the aerosol surface area was reported to be a governing factor for the occurrence of NPF events in Beijing (Cai et al., 2017b).

pSO_4^{2-} is a dominating inorganic compound in particulate matter in sulfur-dominating atmospheric environments, and its origin is mainly secondary processes, especially during haze events (Huang et al., 2014; Zheng et al., 2015a). In the UK, France, and German, pSO_4^{2-} between 1980 and 2000 decreased by 50-70% in response to a 90% reduction in atmospheric SO_2 concentration (Manktelow et al., 2007). In Eastern USA, pSO_4^{2-} between 1989 and 1995 decreased by 26% in response to a 35% reduction in SO_2 concentration (Holland et al., 1998). A simulation analysis on Europe and the USA indicates that every 1% decrease in SO_2 emissions will reduce pSO_4^{2-} by 0.65% (Manktelow et al., 2007). Those observed non-linear responses were not well understood. Recent studies have shown high uncertainty of sulfate formation in China (Cheng et al., 2016; Guo et al., 2017; Ma et al., 2018; Shao et al., 2019; Wang et al., 2016). Although some short-term studies have reported decreased pSO_4^{2-} concentration in recent years (Li et al., 2019a; Moch et al., 2018; Shao et al., 2018), more data is needed to examine the long-term change in pSO_4^{2-}.

In this study, we aim to address the following question: How did pSO_4^{2-}, SA, and NPF frequency change as a response to reduced SO_2 concentration in Beijing? Long-term non-refractory submicron particulate matter ($NR\text{-}PM_1$) was measured using a quadrupole aerosol chemical speciation monitor (Q-ACSM) from Dec. 2011 to Mar. 2019 in Beijing. SA concentration was measured in 2008 summer, 2016 spring, and 2018 to 2019. Simulations from the Community Multiscale Air Quality model with a 2-D Volatility Basis Set (CMAQ/2D-VBS) were also used to explore these responses.

2 METHODOLOGY

2.1 Long-term measurements

Long-term measurements were carried out at two urban sites in Beijing. One site (THU site) is located on the top floor of a four-layer building in the campus of Tsinghua University (40°94′N, 116°33′E), with no tall buildings nearby but three cafeterias which are 170-300 m away from the site (Cai and Jiang, 2017; He et al., 2001). The other site (BUCT site) is on the fifth floor of a teaching building at the west campus of Beijing University of Chemical Technology (39°94′N, 116°30′E), surrounded by some commercial and residential tall buildings (Lu et al., 2019). Both of the two sites are at Haidian District, northwest area of Beijing, and are typical urban sites. The distance between the two sites is 7.1 km. Both of the two sites have meteorological stations to measure temperature (*T*), relative humidity (RH), solar radiation (SR), and other routine parameters. For the long-term SO_2 trend, the data from national stations in Beijing were used (Jiang et al., 2015). Detailed items and time-span of measurements at each site were described in the supplementary information (Figure S1). In the following analysis, winter, spring, summer, and autumn are Dec.-Feb., Mar.-May., Jun.-Aug., and Sep.-Nov., respectively.

Chemical compositions of the NR-PM_1, including pSO_4^{2-} and other non-refractory particulate components, were measured using a Q-ACSM (Ng et al., 2011) between Dec. 2011 and Mar. 2019 at the THU site. The sampling interval was 15-30 min. For this analysis, the data were averaged to an hourly resolution. During the sampling periods, an overall of 26 calibrations for ACSM ionization efficiency (IE) was performed following the procedure described by Ng et al., (2011). An average IE and an average relative ionization efficiency for sulfate (RIE_{SO4}) of 6×10^9 and 0.9, respectively, were used. Particle collection efficiency (CE, Figure S2) was calculated using the ammonium nitrate mass fraction (ANMF) method (Middlebrook et al., 2012). Details of the calibrations can be found in the supplementary information. SA concentration from two campaigns and one continuous measurement spanning from 2008 to 2019 was used. The

continuous measurements were at the BUCT site from Jan. 2018 to Mar. 2019, using a nitrate chemical ionization reaction source coupled with a chemical ionization high-resolution time of flight mass spectrometer (HToF-CIMS, Aerodyne Research, Inc). The nitrate reaction source based on the design of Eisele and Tanner (1993) can measure SA down to 10^4 #·cm^{-3} (Bertram et al., 2011; Jokinen et al., 2012; Kürten et al., 2016). The setup and operation of HToF-CIMS were similar to previously described (Lu et al., 2019). The calibration of the instrument followed a previous study (Kürten et al., 2012). One campaign was at the THU site during Mar. 2016 and Apr. 2016 (Cai et al., 2017b), using a home-made corona discharge ionization source coupled with an HToF-CIMS, The detailed design and calibration of the system have been reported previously (Zheng et al., 2015b). The earliest campaign in Beijing (Wang et al., 2013a; Zheng et al., 2011) was during Jun. 2008 and Aug. 2008, on the campus of Peking University, which is within 2 km of THU site, using an atmospheric pressure ion-drift tube with a quadrupole mass spectrometer (AP-ID-CIMS). The operation and calibration have been described elsewhere (Zheng et al., 2010). SO_2 concentration was measured with SO_2 analyzers (Model 43i, Thermo) at all the three sites in parallel with the SA measurements. All the SA data were averaged to a 5-min resolution.

Size distributions of particles between 1 nm and 10 μm were measured in parallel with SA at both the THU and the BUCT site. Sub-5 nm particles were measured using a home-made DEG-SMPS equipped with a specially designed miniature cylindrical differential mobility analyzer (mini-cyDMA) and a core-sampling apparatus (Cai et al., 2017a; Fu et al., 2019; Jiang et al., 2011). Particles between 3 nm and 10 μm were measured using a particle size distribution spectrometer (PSD) (Liu et al., 2016). Time intervals were 5 minutes. Details of the size distribution measurement system can be found elsewhere (Cai et al., 2017b). The size distribution data were used for estimating condensation sink (CS) and also for classifying NPF events.

2.2 Observational analysis of the sources and sinks of SA and pSO_4^{2-}

Sulfur oxidation ratio (SOR) is commonly used to indicate the conversion ratio of SO_2 to pSO_4^{2-} (Wang et al., 2019),

$$SOR = \frac{\left[SO_4^{2-}\right]}{\left[SO_4^{2-}\right] + \left[SO_2\right]} \quad \text{(Eq. 1)}$$

$[SO_4^{2-}]$ and $[SO_2]$ are the molar concentration of pSO_4^{2-} and SO_2. Note that pSO_4^{2-} in this study represents sulfate in NR-PM_1, the calculated SOR might be lower than those calculated using coarse particles or $PM_{2.5}$. Besides secondary conversion in the atmosphere, primary emissions and transport processes can contribute to pSO_4^{2-} and may lead to some uncertainties in the estimated SOR values.

The main source of atmospheric SA is the oxidation of SO_2 by OH radical (Finlayson-Pitts and Pitts, 1999). The main loss of SA is the condensation loss onto preexisting particles. Thus, the change in SA concentration can be written as:

$$\frac{d\left[H_2SO_4\right]}{dt} = k(T) \cdot OH \cdot SO_2 \text{-} SA \cdot CS \quad \text{(Eq. 2)}$$

SA was sufficiently short-lived that its sources and sinks can be assumed to be in pseudo-steady state, then the change in SA concentration is equal to zero:

$$SA\ production\ rate = k \cdot OH \cdot SO_2 = SA\ loss\ rate = SA \cdot CS \quad \text{(Eq. 3)}$$

where CS (s^{-1}) is the condensation sink which was defined as the rate of condensational loss of SA onto preexisting particles (Kulmala et al., 2001; Pirjola et al., 1999). The calculation method of CS was described previously elsewhere (Cai et al., 2017b). The temperature-dependent reaction constant, *k*, is adopted from previous studies (DeMore et al., 1997; Sander et al., 2002). Studies have shown that tropospheric OH concentration has strong linear correlations with solar ultraviolet radiation despite the complex sources (e.g., photolysis of O_3, NO_2, HONO, H_2O_2, and HCHO) and losses (Rohrer and Berresheim, 2006). Here, we used global solar radiation (SR). To limit onto daytime processes, only data when SR is greater than 10 W are used for the analysis.

2.3 Modeling of SA and pSO_4^{2-}

pSO_4^{2-} in $PM_{2.5}$ and SA concentrations in Beijing during 2013, 2015, and 2017 were modeled using the CMAQ/2D-VBS (Leung et al., 2018; Zhao et al., 2018; Zheng et al., 2019). The modeling domain covered East Asia with a grid spacing of 36 × 36 km^2. The anthropogenic emission inventories used in the simulations were developed by Zhao et al. (2018) and Ding et al. (2019). The meteorological fields for input into the CMAQ/2D-VBS model were simulated by the Weather Research and Forecasting Model (WRF) v3.7. The configurations of WRF and CMAQ/2D-VBS have been described in previous studies (Leung et al., 2018; Zhao et al., 2018; Zheng et al., 2019). We compared the CMAQ/2D-VBS simulation results with surface observations of O_3, $PM_{2.5}$, major chemical components of $PM_{2.5}$, and satellite retrievals of aerosol optical depth (AOD) and NO_2 column density. The simulated magnitude and temporal trends of these pollutants agree reasonably well with observations (Leung et al., 2018; Zhao et al., 2018).

3. RESULTS AND DISCUSSION

3.1 Response of particulate sulfate

pSO_4^{2-} and its fraction in NR-PM_1 declined with fluctuations in response to reduced SO_2 concentrations during 2012 and 2019 (Figure 1). The average SO_2 concentration decreased from an annual average of 9.1 ppb in 2013 to an annual average of 1.7 ppb in 2018 (Figure 1a). The reduction rate during the six years was 81%. The meteorological conditions (RH, T, and SR) in different years (2012-2019) were comparable to each other (Figure S3). The concentration of pSO_4^{2-} decreased with fluctuations from ~10 $\mu g \cdot m^{-3}$ during 2012-2014 to ~4 $\mu g \cdot m^{-3}$ during 2017-2019 (Figure 1b). The reduction rate was ~60%. The modeled pSO_4^{2-} (in $PM_{2.5}$) reduction trend agreed well with the measured pSO_4^{2-} (in NR-PM_1). The mass fraction of pSO_4^{2-} in NR-PM_1 decreased from ~20-30% in 2012 to less than 10% in 2019 (Figure 1c). pSO_4^{2-} in Beijing is mainly from secondary formation, with a nonnegligible fraction from primary emissions (Huang et al., 2014; Shao et al., 2019). Therefore, the reduction of pSO_4^{2-} should be attributed to a combined effect of reductions in

secondary formation from SO_2 and primary emissions of pSO_4^{2-}. The decreased pSO_4^{2-} fraction in NR-PM_1 is in accordance with the fact that SO_2 and particulate matter are the most significantly reduced pollutants, as compared to NO_x, NH_3, and VOCs (Cheng et al., 2019; Zheng et al., 2018).

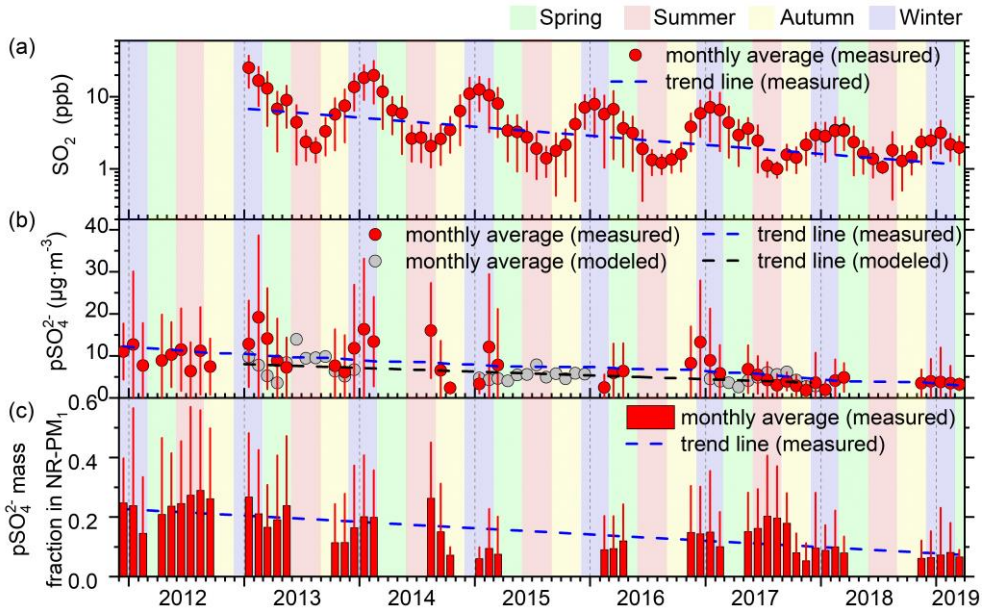

Figure 1. (a) Monthly average SO_2 concentrations in Beijing from Jan. 2013 to Mar. 2019. The data is the average from twelve national monitoring stations in Beijing (Jiang et al., 2015). (b) Monthly average pSO_4^{2-} concentrations in NR-PM_1 measured using the Q-ACSM from Dec. 2011 to Mar. 2019. Grey points are the simulated pSO_4^{2-} in $PM_{2.5}$ using CMAQ/2D-VBS. (c) Corresponding monthly pSO_4^{2-} mass fraction in NR-PM_1. The red lines in the three subplots represent the standard deviations of the data. The blue dashed lines are the trend lines obtained by linear regression of the measured data. The black dashed line is the trend line obtained by linear regression of the simulated data.

Non-linear reduction in pSO_4^{2-} with the reduced SO_2 concentration was observed, as indicated by increased SOR during 2013 and 2019 (Figure 2). Firstly, SOR in different seasons were significantly different: the highest SOR was observed in summer, with an average of ~0.4, nearly twice as that in winter. The distinct seasonal variation was also captured by the CMAQ/2D-VBS model. The higher SOR in summer was a combined effect of higher RH, higher T, and higher atmospheric oxidation capability (Figure S3 & S4). Average SOR in wintertime and springtime increased

from an average of ~0.15 in 2012-2013 to an average of ~0.19 in 2018-2019. This indicated a non-linear relationship between reduced pSO_4^{2-} and SO_2 concentrations. Due to the limited data points, no clear long-term trend on SOR change during summer and autumn can be concluded. The modeled SOR also showed increasing trends from 2013 to 2017. Considering that the measured and modeled SOR were calculated from pSO_4^{2-} in NR-PM_1 and $PM_{2.5}$, respectively, and the measured results represent the situation at the measuring site while the modeled results represent a larger space in Beijing, however, the exact values cannot be directly compared. Besides, previous studies have reported underestimation of modeled SOR due to missing or underestimated pathways for pSO_4^{2-} formation in the CMAQ model (Cheng et al., 2016; Sarwar et al., 2013; Shao et al., 2019) and overestimation of measured pSO_4^{2-} due to the misinterpret of some organosulfur compounds (Moch et al., 2018; Song et al., 2019a).

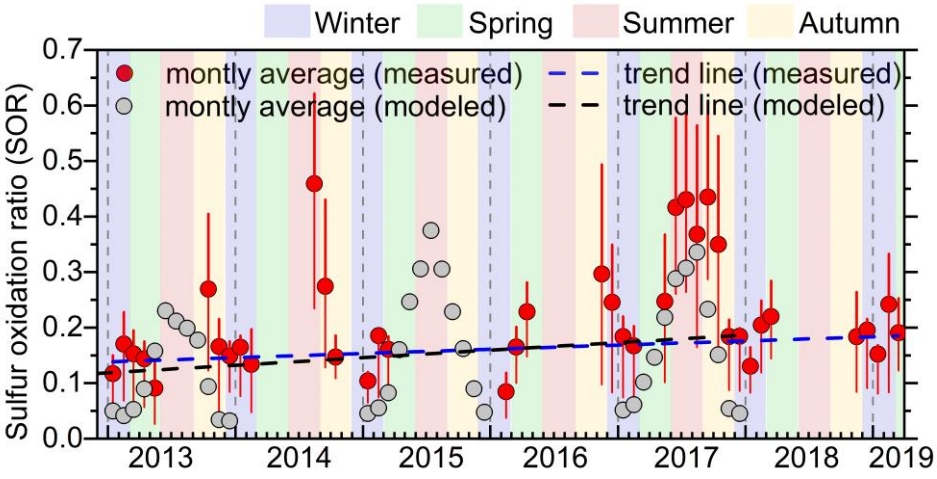

Figure 2. Measured (red points) and CMAQ/2D-VBS simulated (grey points) monthly average sulfur oxidation ratio (SOR = $[pSO_4^{2-}]$ / ($[pSO_4^{2-}]$ + $[SO_2]$)). The end of the red lines represents the 25th and 75th percentiles. The blue dashed line is the trend line obtained by linear regression of the measured data. The black dashed line is the trend line obtained by linear regression of the simulated data.

Based on the CMAQ/2D-VBS simulation results, the increased SOR was mainly attributed to the increased O_3 and OH concentrations. Firstly, the simulated SOR has good positive correlations with O_3 and OH concentrations (Figure 3a-b), which indicates that O_3 and OH are good representations of the SO_2 oxidants in the CMAQ/2D-VBS model. The

simulated O_3 concentrations increased from 26.1 ppb in 2013 to 31.4 ppb in 2017, the simulated OH increased from 1.3×10^6 #·cm^3 in 2013 to 1.7×10^6 #·cm^3 in 2017, and the simulated SOR increased from 0.11 in 2013 to 0.17 in 2017. The increases in oxidants were most significant in winter (Figure S4). Previous studies also indicated increased atmospheric oxidation capability during 2013 and 2017 in Chinese megacity clusters (Li et al., 2019b). Secondly, as shown in Figure 3a and 3b, under similar O_3 or OH concentrations, SOR was slightly higher for low SO_2 concentrations, which may be explained by the relatively more sufficient oxidation capacity under low SO_2 concentrations. The increased SOR should not be caused by the meteorological conditions in different years as when we fixed the meteorological conditions as the same with year 2015 in the CMAQ/2D-VBS model, the SOR increasing trend is similar (Figure S5).

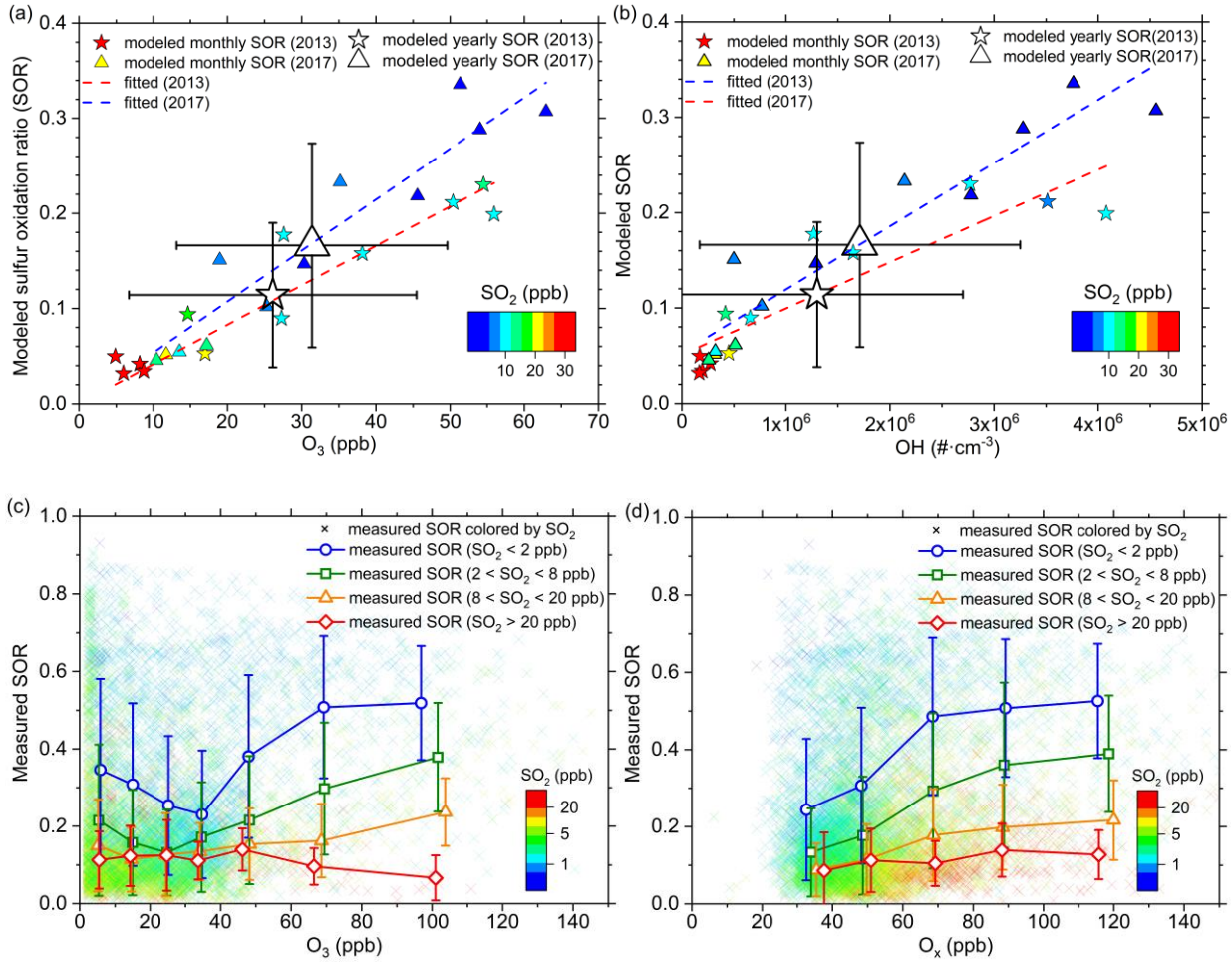

Figure 3. The modeled monthly and yearly sulfur oxidation ratio (SOR = $[pSO_4^{2-}]$ / ($[pSO_4^{2-}]$ + $[SO_2]$)) as a function of (a) O_3 concentration and (b) OH concentration colored by SO_2 concentration; the measured hourly SOR as a function of (c) O_3 concentration and (d) Ox (O_3+NO_2) concentration colored by SO_2 concentration.

However, reasons for the increased SOR are probably more complicated, possibly be a combined effect from the increased oxidants (e.g., O_3), relatively more sufficient oxidation capacity under reduced SO_2 concentrations, and other possible factors (e.g., increased NH_3 concentrations). Figure 3c shows all the measured hourly average SOR as a function of O_3 concentration. Firstly, SOR generally increased with O_3 concentrations when O_3 was high and SO_2 was low. The measured O_3 increased slightly from an annual average of 20.3 ppb in 2013 to an annual average of 28.0 ppb in 2018, as shown in Figure S4. As a result, the measured increase in SOR from 2013 to 2018 could be introduced by increased O_3 concentration. However, under low O_3 concentrations or high SO_2 concentrations, the positive correlation between SOR and O_3 did not exist, which was not expected by the model. A possible reason is that the reliance of SOR on O_3 was interfered by its reliance on RH, which is another important factor for SOR (Cheng et al., 2016; Wang et al., 2016; Zhang et al., 2019). Another possibility is that other important oxidants, like NO_2, take the dominating role in oxidizing SO_2 under low O_3 and high SO_2 concentrations. As shown in Figure 3d, SOR has a better correlation with O_x (odd oxygen: O_3+NO_2) than O_3. Recent studies have emphasized the importance of NO_2 on the oxidation of SO_2 under high NO_2, high NH_3, high RH, and sometimes high dust aerosol concentrations in Beijing (Cheng et al., 2016; Wang et al., 2016; Zhang et al., 2019). However, this pathway has not been integrated into the current CMAQ/2D-VBS model because of the high uncertainty introduced by its high reliability on particle pH. However, neither RH nor O_x had a long-term increasing trend, which could not be the reason for the long-term increase in SOR. Secondly, under similar O_3 concentrations, SOR was significantly higher under low SO_2 (SOR = 0.37 for SO_2 < 2 ppb) than high SO_2 concentrations (SOR = 0.11 for SO_2 > 20 ppb), this can be explained by the relatively more sufficient oxidation capacity under low SO_2 concentrations, consistent with the simulated results. Thirdly, previous studies have reported

increased particle pH due to the relatively more abundant NH_3, the increased pH would facilitate the heterogeneous formation of pSO_4^{2-} and thus increase SOR (Fu et al., 2017; Song et al., 2019b). Thus, the increased O_3 concentrations, the relatively more sufficient oxidation capacity under low SO_2 concentrations, and possibly the relatively more abundant NH_3 can play a synergistic role in elevating SOR.

3.2 Response of sulfuric acid

No dramatic change in SA concentration was observed in response to the decreased SO_2 trend (Figure 4). Average SO_2 during the four measuring periods in Beijing from 2008 to 2019 were 4.1, 5.8, 4.2, 2.5 ppb. However, no dramatic change in SA concentration was observed, with the average concentration during the four periods being 2.4×10^6, 5.6×10^5, 4.5×10^6, and 2.0×10^6 #·cm^{-3}, respectively. Note that the SA measurements were relatively scarce and spread in different seasons, thus we cannot exclude the possibility that SA concentration presented in this analysis did not catch the long-term trend. The ongoing continuous SA measurement at the BUCT site will help to further address this. When comparing Beijing with other sites around the world (Figure 4), SO_2 in Beijing and Atlanta (both urban sites) was significantly higher than the rural and forest sites. However, SA concentrations in the urban sites were comparable to those in the rural and forest sites.

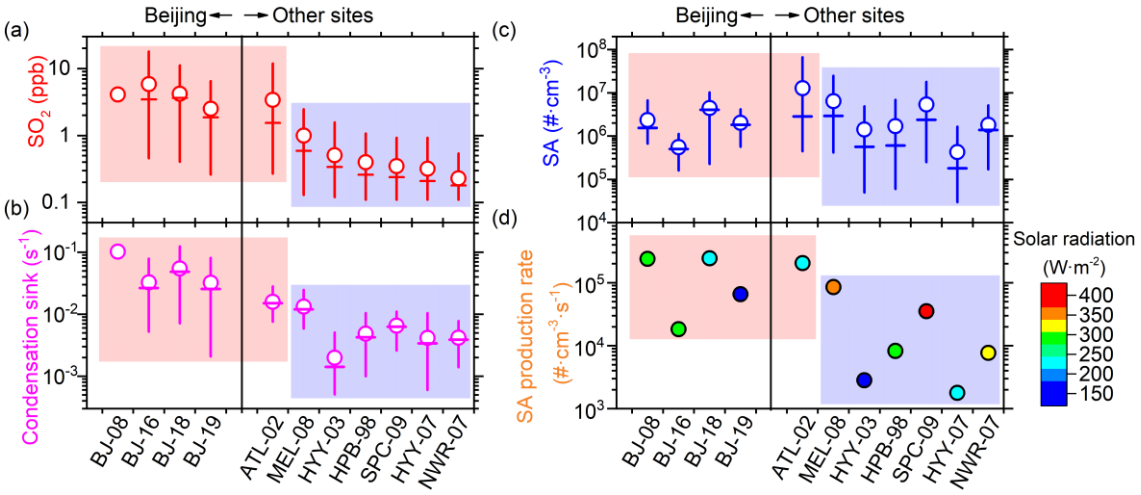

Figure 4. The average, 5th, 50th, and 95th percentiles of (a) SO_2, (b) condensation sink (CS), and (c) SA concentration, during four periods in

Beijing (BJ) and other sites of the world (Mikkonen et al., 2011), including Atlanta, Georgia, USA (ATL), Melpitz, Germany (MEL), Hyytiälä, Finland (HYY), Hohenpeissenberg, Germany (HPB), San Pietro Capofiume, Italy (SPC), Niwot Ridge, Colorado, USA (NWR). (d) The average SA production rate for Beijing and other sites. The red shaded area includes urban sites, the blue shaded area includes rural and forest sites.

When putting all the 5-min average sampling data together (Figure S7), we observed that the apparent SA conversion ratio (SA:SO_2 molar ratio) increased significantly from ~0.001% to ~1% as SO_2 decreased from 10 ppb to 0.01 ppb. This increase in SA:SO_2 ratio in response to reduced SO_2 concentration was also observed in the CMAQ/2D-VBS simulation results. The increased apparent conversion ratio indicated that the response of SA concentration to SO_2 is non-linear. One reason for the non-linear response is that the sulfuric acid concentration is often limited by the oxidants, rather than SO_2 concentration. That is, the oxidants to form SA became more sufficient in reduced SO_2 concentrations.

Decreased CS was one of the reasons for the relatively stable SA concentration and the increased SA:SO_2 under reduced SO_2 concentrations. CS during the four periods in Beijing was 0.102, 0.033, 0.055, and 0.032 s^{-1}, respectively. It has a decreasing trend. As a result, the reduced SA production (due to reduced SO_2) and the reduced loss rate (due to reduced CS) may cancel out to some extent and result in stable SA concentrations in Beijing. Similarly, CS and the SA loss rate (SA·CS) in the clean rural and forest sites is significantly lower than the urban sites (Figure 4), which buffered the difference in SA concentration in different sites by reducing SA loss rate. When looking at the 5-min average data points in Beijing (Figure 5a), a clear influence from CS was observed on SA:SO_2 molar ratio. SA:SO_2 under CS < 0.02 s^{-1} can be one magnitude higher than those under CS > 0.05 s^{-1}.

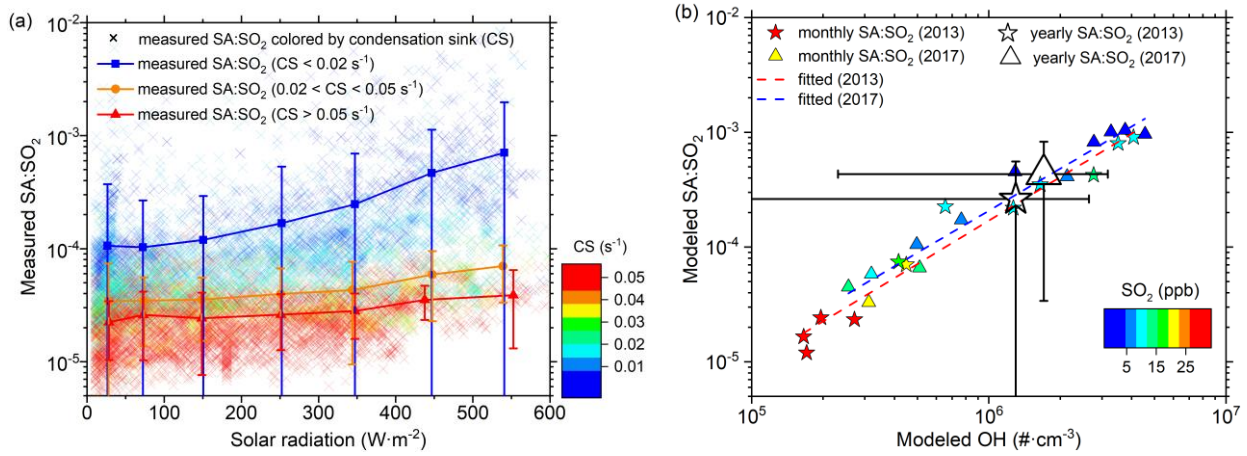

Figure 5. (a) The apparent SA conversion ratio (SA:SO_2 molar ratio) as a function of solar radiation colored by condensation sink (CS) in Beijing. (b) The CMAQ/2D-VBS simulated monthly SA:SO_2 as a function of modeled OH concentrations.

The increased atmospheric oxidation capacity may also play a minor role in the relatively constant SA concentration and the increased SA:SO_2 ratio with reduced SO_2 concentration. In Figure 5a, a positive correlation between measured SA:SO_2 with solar radiation, which has a good positive relationship with OH concentration, can be observed. The positive correlation is stronger under low CS. While in the CMAQ/2D-VBS model, SA:SO_2 relies radically on OH concentration, as indicated by the good linearity between SA:SO_2 and OH concentration in Figure 5b. The modeled OH concentrations increased from 1.3×10^6 #·cm^{-3} in 2013 to 1.7×10^6 #·cm^{-3} in 2017, and the SA:SO_2 molar ratio increased from 2.6×10^{-4} #·cm^{-3} in 2013 to 4.3×10^{-4} #·cm^{-3} in 2017. When comparing different sites, one can assume pseudo-steady state and that all SA is formed via OH oxidation. If so, the OH concentrations required to explain the observed SA concentration in the urban area (10^5-10^7 #·cm^{-3}) is one magnitude higher than in rural and forest sites (10^4-10^6 #·cm^{-3}) as shown in Figure S6. These OH concentrations were in the same range as our modeled results in Beijing (Figure S4) and those observed in the urban and rural areas (Petaja et al., 2009; Rohrer and Berresheim, 2006).

3.3 Variations of NPF frequency

Despite its seasonal variations, the NPF frequency in Beijing remains relatively constant from 2004 to 2019 (Figure 6). NPF frequency in 2018 was 41%, based on our one-year measurement. This frequency is close to 40% in 2004 and 43%

in 2008 (Shen et al., 2011; Wang et al., 2013b; Wu et al., 2007). The stable NPF frequency in Beijing is in good agreement with the relatively stable SA concentrations. However, the occurrence of NPF is also influenced by other factors such as CS and gaseous precursors such as NH_3 and amines (Cai et al., 2017b; Kerminen et al., 2018; Wang et al., 2011b). The constant NPF frequency in Beijing is different from that at eastern Lapland, Finland (Kyro et al., 2014), Melpitz, Germany (Hamed et al., 2010), and Pittsburgh, USA (Saha et al., 2018), where NPF frequency and NPF strength decreased significantly with decreased SO_2 concentration. Revealing the governing factor for NPF events at different sites are needed to understand the observed differences.

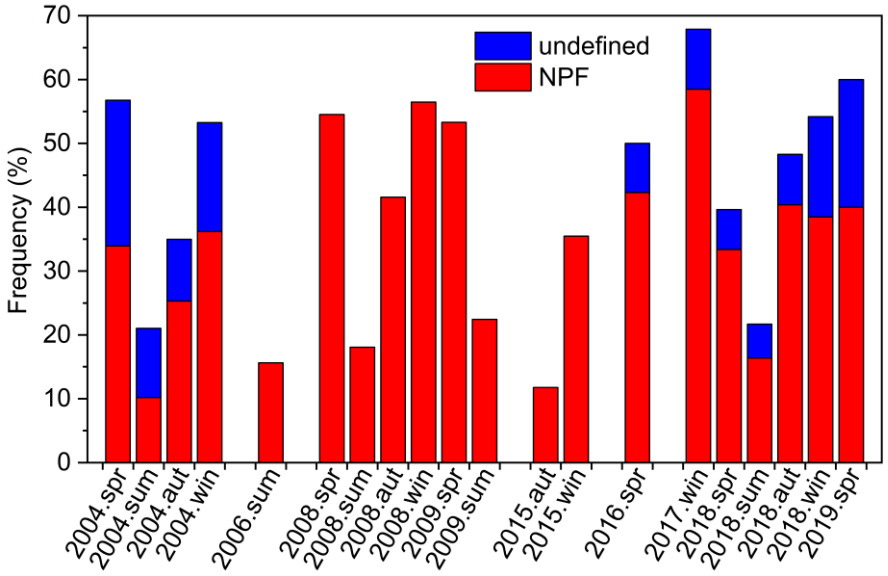

Figure 6. The variations of NPF frequency (fraction of days having NPF) in different seasons in Beijing during 2004-2019. Data from Jan. 2018 to Mar. 2019 is measured in our study. Data from other years are from previous studies (Cai et al., 2017b; Jayaratne et al., 2017; Shen et al., 2011; Wang et al., 2013b; Wu et al., 2007; Yue et al., 2009). A day is classified as an NPF day if there is a burst of sub-3 nm particles that follows with subsequent particle growth. While a day is classified as an "undefined" day if the burst of particles does not follow with the subsequent growth.

Clear seasonal variations of NPF frequency were observed in Beijing, with the highest frequency in winter (50-70%) and lowest in summer (10-25%). The lowest NPF frequency in summer is possibly due to the evaporation of those clusters

critical for NPF because of high temperatures. This seasonal variation is also different from other sites around the world, like Finland and German, where NPF frequency is highest in summer when solar radiation is the strongest (Dada et al., 2017; Hamed et al., 2010; Kyro et al., 2014).

4 CONCLUSION

With the SO_2 concentration in Beijing decreased from an annual average of 9.1 ppb in 2013 to an annual average of 1.7 ppb in 2018, the concentration of particulate sulfate decreased with fluctuations from ~10 $\mu g \cdot m^{-3}$ in 2012-2013 to ~4 $\mu g \cdot m^{-3}$ in 2018-2019. The 81% reduction in SO_2 resulted in a ~60% reduction in particulate sulfate. This non-linear response of particulate sulfate to SO_2 concentration was supported by a slight increase in sulfur oxidation ratio from 2013 to 2019, which was also observed in the CMAQ/2D-VBS simulations. The increased sulfur oxidation ratio with reduced SO_2 concentration can be attributed to the relatively more sufficient oxidation capability under low SO_2 concentration and a slight increase in atmospheric oxidation capability (e.g., increased O_3 and OH concentrations), as indicated by both measurements and CMAQ/2D-VBS simulations. Other factors, like the increasing NH_3 concentration, may also play a role.

Based on data from several measuring periods from 2008 to 2019, sulfuric acid concentrations remained relatively stable. Bulk sulfuric acid apparent conversion ratio ($SA:SO_2$) decreased with increased SO_2 concentration. This was supported by the CMAQ/2D-VBS simulations. This might be due to the decreased condensation sink which buffered the decrease in sulfuric acid concentration. The slightly increased atmospheric oxidation capacity may also play a role. Despite its relatively high SO_2 concentration, sulfuric acid concentration in Beijing is in a similar range with sites in other countries, also because of a buffering effect from high condensation sink. The new particle formation frequency remains relatively constant during 2004 and 2019, consistent with the relatively stable sulfuric acid concentration. Continuous long-term measurement of sulfuric acid, OH radical, amine, NH_3, low volatile organics, and particulate molecular compositions

will be helpful to further address the response of secondary formation processes to the strict air pollution control actions in China.

Acknowledgments

Financial support from the National Key R&D Program of China (2017YFC0209503), the National Natural Science Foundation of China (91643201, 21625701) is acknowledged.

References

Bertram, T. H., Kimmel, J. R., Crisp, T. A., Ryder, O. S., Yatavelli, R. L. N., Thornton, J. A., Cubison, M. J., Gonin, M., and Worsnop, D. R.: A field-deployable, chemical ionization time-of-flight mass spectrometer, Atmos Meas Tech, 4, 1471-1479, 2011.

Birmili, W., and Wiedensohler, A.: New particle formation in the continental boundary layer: Meteorological and gas phase parameter influence, Geophys Res Lett, 27, 3325-3328, 10.1029/1999gl011221, 2000.

Birmili, W., Berresheim, H., Plass-D¨¹lmer, C., and Elste, T.: The Hohenpeissenberg aerosol formation experiment (HAFEX): a long-term study including size-resolved aerosol, H2SO4, OH, and monoterpenes measurements, Atmospheric Chemistry and Physics (ACP) & Discussions (ACPD), 2003.

Cai, R., Chen, D.-R., Hao, J., and Jiang, J.: A miniature cylindrical differential mobility analyzer for sub-3 nm particle sizing, J Aerosol Sci, 106, 111-119, 10.1016/j.jaerosci.2017.01.004, 2017a.

Cai, R., and Jiang, J.: A new balance formula to estimate new particle formation rate: reevaluating the effect of coagulation scavenging, Atmos Chem Phys, 17, 12659-12675, 2017.

Cai, R., Yang, D., Fu, Y., Wang, X., Li, X., Ma, Y., Hao, J., Zheng, J., and Jiang, J.: Aerosol surface area concentration: a governing factor in new particle formation in Beijing, Atmos Chem Phys, 17, 12327, 2017b.

Cheng, J., Su, J., Cui, T., Li, X., Dong, X., Sun, F., Yang, Y., Tong, D., Zheng, Y., Li, Y., Li, J., Zhang, Q., and He, K.: Dominant role of emission reduction in PM2.5 air quality improvement in Beijing during 2013-2017: a model-based decomposition analysis, Atmos Chem Phys, 19, 6125-6146, 10.5194/acp-19-6125-2019, 2019.

Cheng, Y., Zheng, G., Wei, C., Mu, Q., Zheng, B., Wang, Z., Gao, M., Zhang, Q., He, K., and Carmichael, G.: Reactive nitrogen chemistry in aerosol water as a source of sulfate during haze events in China, Science advances, 2, e1601530, 2016.

Chu, B., Kerminen, V.-M., Bianchi, F., Yan, C., Petaja, T., and Kulmala, M.: Atmospheric new particle formation in China, Atmos Chem Phys, 19, 115-138, 10.5194/acp-19-115-2019, 2019.

Dada, L., Paasonen, P., Nieminen, T., Buenrostro Mazon, S., Kontkanen, J., Peräkylä, O., Lehtipalo, K., Hussein, T., Petäjä, T., and Kerminen, V.-M.: Long-term analysis of clear-sky new particle formation events and nonevents in Hyytiälä, Atmos Chem Phys, 17, 6227-6241, 2017.

DeMore, W., Sander, S., Golden, D., Hampson, R., Kurylo, M., Howard, C., Ravishankara, A., Kolb, C., and Molina, M.: Chemical kinetics and photochemical data for use in stratospheric modeling, 94-94，266, 1997.

Ding, D., Xing, J., Wang, S., Liu, K., and Hao, J.: Estimated Contributions of Emissions Controls, Meteorological Factors, Population Growth, and Changes in Baseline Mortality to Reductions in Ambient PM2.5 and PM2.5-Related Mortality in

China, 2013-2017, Environmental Health Perspectives, 127, 10.1289/ehp4157, 2019.
Eisele, F. L., and Tanner, D. J.: Measurement of the gas-phas concentration of H2SO4 and methane sulfonic-acid and estimates of H2SO4 production and loss in the atmosphere, J Geophys Res-Atmos, 98, 9001-9010, 10.1029/93jd00031, 1993.
Finlayson-Pitts, B. J., and Pitts, J. N.: Chemistry of the upper and lower atmosphere : theory, experiments and applications, Academic Press, San Diego, Calif., 969 pp., 1999.
Fu, X., Wang, S., Xing, J., Zhang, X., Wang, T., and Hao, J.: Increasing Ammonia Concentrations Reduce the Effectiveness of Particle Pollution Control Achieved via SO2 and NO X Emissions Reduction in East China, Environ Sci Tech Let, 4, 221-227, 2017.
Fu, Y., Xue, M., Cai, R., Kangasluoma, J., and Jiang, J.: Theoretical and experimental analysis of the core sampling method: Reducing diffusional losses in aerosol sampling line, Aerosol Sci Tech, 53, 793-801, 10.1080/02786826.2019.1608354, 2019.
Guo, H., Weber, R. J., and Nenes, A.: High levels of ammonia do not raise fine particle pH sufficiently to yield nitrogen oxide-dominated sulfate production, Scientific reports, 7, 12109, 2017.
Guo, S., Hu, M., Zamora, M. L., Peng, J., Shang, D., Zheng, J., Du, Z., Wu, Z., Shao, M., and Zeng, L.: Elucidating severe urban haze formation in China, Proceedings of the National Academy of Sciences, 111, 17373-17378, 2014.
Hamed, A., Birmili, W., Joutsensaari, J., Mikkonen, S., Asmi, A., Wehner, B., Spindler, G., Jaatinen, A., Wiedensohler, A., Korhonen, H., Lehtinen, K. E. J., and Laaksonen, A.: Changes in the production rate of secondary aerosol particles in Central Europe in view of decreasing SO₂ emissions between 1996 and 2006, Atmos. Chem. Phys., 10, 1071-1091, 10.5194/acp-10-1071-2010, 2010.
He, K., Yang, F., Ma, Y., Zhang, Q., Yao, X., Chan, C. K., Cadle, S., Chan, T., and Mulawa, P.: The characteristics of PM2. 5 in Beijing, China, Atmos Environ, 35, 4959-4970, 2001.
Holland, D. M., Principe, P. P., and Sickles, J. E.: Trends in atmospheric sulfur and nitrogen species in the eastern United States for 1989-1995, Atmos Environ, 33, 37-49, 1998.
Huang, R.-J., Zhang, Y., Bozzetti, C., Ho, K.-F., Cao, J.-J., Han, Y., Daellenbach, K. R., Slowik, J. G., Platt, S. M., and Canonaco, F.: High secondary aerosol contribution to particulate pollution during haze events in China, Nature, 514, 218-222, 2014.
Jaatinen, A., Hamed, A., Joutsensaari, J., Mikkonen, S., Birmili, W., Wehner, B., Spindler, G., Wiedensohler, A., Decesari, S., Mircea, M., Facchini, M. C., Junninen, H., Kulmala, M., Lehtinen, K. E. J., and Laaksonen, A.: A comparison of new particle formation events in the boundary layer at three different sites in Europe, Boreal Environ Res, 14, 481-498, 2009.
Jayaratne, R., Pushpawela, B., He, C., Li, H., Gao, J., Chai, F., and Morawska, L.: Observations of particles at their formation sizes in Beijing, China, Atmos Chem Phys, 17, 8825-8835, 10.5194/acp-17-8825-2017, 2017.
Jiang, J., Chen, M., Kuang, C., Attoui, M., and McMurry, P. H.: Electrical mobility spectrometer using a diethylene glycol condensation particle counter for measurement of aerosol size distributions down to 1 nm, Aerosol Sci Tech, 45, 510-521, 2011.
Jiang, J., Zhou, W., Cheng, Z., Wang, S., He, K., and Hao, J.: Particulate Matter Distributions in China during a Winter Period with Frequent Pollution Episodes (January 2013), Aerosol Air Qual Res, 15, 494-U157, 10.4209/aaqr.2014.04.0070, 2015.
Jokinen, T., Sipila, M., Junninen, H., Ehn, M., Lonn, G., Hakala, J., Petaja, T., Mauldin, R. L., Kulmala, M., and Worsnop, D. R.: Atmospheric sulphuric acid and neutral cluster measurements using CI-APi-TOF, Atmos Chem Phys, 12, 4117-4125, 2012.
Kerminen, V.-M., Chen, X., Vakkari, V., Petaja, T., Kulmala, M., and Bianchi, F.: Atmospheric new particle formation and growth: review of field observations, Environ Res Lett, 13, 10.1088/1748-9326/aadf3c, 2018.
Kuang, C., McMurry, P. H., McCormick, A. V., and Eisele, F. L.: Dependence of nucleation rates on sulfuric acid vapor concentration in diverse atmospheric locations, J Geophys Res, 113, 10.1029/2007jd009253, 2008.
Kulmala, M., Dal Maso, M., Makela, J. M., Pirjola, L., Vakeva, M., Aalto, P., Miikkulainen, P., Hameri, K., and O'Dowd, C. D.: On the formation, growth and composition of nucleation mode particles, Tellus B, 53, 479-490, 10.1034/j.1600-0889.2001.d01-33.x, 2001.
Kürten, A., Rondo, L., Ehrhart, S., and Curtius, J.: Calibration of a Chemical Ionization Mass Spectrometer for the Measurement of Gaseous Sulfuric Acid, J Phys Chem A, 116, 6375-6386, 2012.
Kürten, A., Bergen, A., Heinritzi, M., Leiminger, M., Lorenz, V., Piel, F., Simon, M., Sitals, R., Wagner, A. C., and Curtius, J.:

Observation of new particle formation and measurement of sulfuric acid, ammonia, amines and highly oxidized organic molecules at a rural site in central Germany, Atmos Chem Phys, 16, 12793-12813, 10.5194/acp-16-12793-2016, 2016.
Kyro, E. M., Vaananen, R., Kerminen, V. M., Virkkula, A., Petaja, T., Asmi, A., Dal Maso, M., Nieminen, T., Juhola, S., Shcherbinin, A., Riipinen, I., Lehtipalo, K., Keronen, P., Aalto, P. P., Hari, P., and Kulmala, M.: Trends in new particle formation in eastern Lapland, Finland: effect of decreasing sulfur emissions from Kola Peninsula, Atmos Chem Phys, 14, 4383-4396, 10.5194/acp-14-4383-2014, 2014.
Leung, D. M., Tai, A. P. K., Mickley, L. J., Moch, J. M., van Donkelaar, A., Shen, L., and Martin, R. V.: Synoptic meteorological modes of variability for fine particulate matter (PM2.5) air quality in major metropolitan regions of China, Atmos Chem Phys, 18, 6733-6748, 10.5194/acp-18-6733-2018, 2018.
Li, H., Cheng, J., Zhang, Q., Zheng, B., Zhang, Y., Zheng, G., and He, K.: Rapid transition in winter aerosol composition in Beijing from 2014 to 2017: response to clean air actions, Atmos Chem Phys, 19, 11485-11499, 10.5194/acp-19-11485-2019, 2019a.
Li, K., Jacob, D. J., Liao, H., Shen, L., Zhang, Q., and Bates, K. H.: Anthropogenic drivers of 2013-2017 trends in summer surface ozone in China, P Natl Acad Sci USA, 116, 422-427, 10.1073/pnas.1812168116, 2019b.
Liu, J., Jiang, J., Zhang, Q., Deng, J., and Hao, J.: A spectrometer for measuring particle size distributions in the range of 3 nm to 10 μm, Frontiers of Environmental Science & Engineering, 10, 63-72, 2016.
Lu, Y., Yan, C., Fu, Y., Chen, Y., Liu, Y., Yang, G., Wang, Y., Bianchi, F., Chu, B., Zhou, Y., Yin, R., Baalbaki, R., Garmash, O., Deng, C., Wang, W., Liu, Y., Petaja, T., Kerminen, V.-M., Jiang, J., Kulmala, M., and Wang, L.: A proxy for atmospheric daytime gaseous sulfuric acid concentration in urban Beijing, Atmos Chem Phys, 19, 1971-1983, 10.5194/acp-19-1971-2019, 2019.
Ma, J., Chu, B., Liu, J., Liu, Y., Zhang, H., and He, H.: NOx promotion of SO2 conversion to sulfate: An important mechanism for the occurrence of heavy haze during winter in Beijing, Environ Pollut, 233, 662-669, 10.1016/j.envpol.2017.10.103, 2018.
Manktelow, P. T., Mann, G. W., Carslaw, K. S., Spracklen, D. V., and Chipperfield, M. P.: Regional and global trends in sulfate aerosol since the 1980s, Geophys Res Lett, 34, 10.1029/2006gl028668, 2007.
Middlebrook, A. M., Bahreini, R., Jimenez, J. L., and Canagaratna, M. R.: Evaluation of Composition-Dependent Collection Efficiencies for the Aerodyne Aerosol Mass Spectrometer using Field Data, Aerosol Sci Tech, 46, 258-271, 10.1080/02786826.2011.620041, 2012.
Mikkonen, S., Romakkaniemi, S., Smith, J. N., Korhonen, H., Petaja, T., Plass-Duelmer, C., Boy, M., McMurry, P. H., Lehtinen, K. E. J., Joutsensaari, J., Hamed, A., Mauldin, R. L., III, Birmili, W., Spindler, G., Arnold, F., Kulmala, M., and Laaksonen, A.: A statistical proxy for sulphuric acid concentration, Atmos Chem Phys, 11, 11319-11334, 10.5194/acp-11-11319-2011, 2011.
Moch, J. M., Dovrou, E., Mickley, L. J., Keutsch, F. N., Cheng, Y., Jacob, D. J., Jiang, J., Li, M., Munger, J. W., Qiao, X., and Zhang, Q.: Contribution of Hydroxymethane Sulfonate to Ambient Particulate Matter: A Potential Explanation for High Particulate Sulfur During Severe Winter Haze in Beijing, Geophys Res Lett, 45, 11969-11979, 10.1029/2018gl079309, 2018.
Ng, N. L., Herndon, S. C., Trimborn, A., Canagaratna, M. R., Croteau, P. L., Onasch, T. B., Sueper, D., Worsnop, D. R., Zhang, Q., Sun, Y. L., and Jayne, J. T.: An Aerosol Chemical Speciation Monitor (ACSM) for Routine Monitoring of the Composition and Mass Concentrations of Ambient Aerosol, Aerosol Sci Tech, 45, 780-794, 2011.
Perraud, V., Horne, J. R., Martinez, A. S., Kalinowski, J., Meinardi, S., Dawson, M. L., Wingen, L. M., Dabdub, D., Blake, D. R., Gerber, R. B., and Finlayson-Pitts, B. J.: The future of airborne sulfur-containing particles in the absence of fossil fuel sulfur dioxide emissions, P Natl Acad Sci USA, 112, 13514-13519, 10.1073/pnas.1510743112, 2015.
Petaja, T., Mauldin, R. L., III, Kosciuch, E., McGrath, J., Nieminen, T., Paasonen, P., Boy, M., Adamov, A., Kotiaho, T., and Kulmala, M.: Sulfuric acid and OH concentrations in a boreal forest site, Atmos Chem Phys, 9, 7435-7448, 10.5194/acp-9-7435-2009, 2009.
Pirjola, L., Kulmala, M., Wilck, M., Bischoff, A., Stratmann, F., and Otto, E.: Formation of sulphuric acid aerosols and cloud condensation nuclei: An expression for significant nucleation and model comparison, J Aerosol Sci, 30, 1079-1094, 10.1016/s0021-8502(98)00776-9, 1999.
Rohrer, F., and Berresheim, H.: Strong correlation between levels of tropospheric hydroxyl radicals and solar ultraviolet

radiation, Nature, 442, 184-187, 10.1038/nature04924, 2006.
Saha, P. K., Robinson, E. S., Shah, R. U., Zimmerman, N., Apte, J. S., Robinson, A. L., and Presto, A. A.: Reduced Ultrafine Particle Concentration in Urban Air: Changes in Nucleation and Anthropogenic Emissions, Environ Sci Technol, 52, 6798-6806, 10.1021/acs.est.8b00910, 2018.
Sander, S. P., Friedl, R. R., Golden, D. M., Kurylo, M. J., Huie, R. E., Orkin, V. L., Ravishankara, A. R., Kolb, C. E., and Molina, M. J.: Chemical kinetics and photochemical data for use in stratospheric modeling, in, 2002.
Sarwar, G., Fahey, K., Kwok, R., Gilliam, R. C., Roselle, S. J., Mathur, R., Xue, J., Yu, J., and Carter, W. P. L.: Potential impacts of two SO2 oxidation pathways on regional sulfate concentrations: Aqueous-phase oxidation by NO2 and gas-phase oxidation by Stabilized Criegee Intermediates, Atmos Environ, 68, 186-197, 10.1016/j.atmosenv.2012.11.036, 2013.
Seinfeld, J. H., and Pandis, S. N.: Atmospheric Chemistry and Physics-From Air Pollution to Climate Change, 2nd ed., John Wiley & Sons: Hoboken, NJ, 2006.
Shao, J., Chen, Q., Wang, Y., Lu, X., He, P., Sun, Y., Shah, V., Martin, R. V., Philip, S., Song, S., Zhao, Y., Xie, Z., Zhang, L., and Alexander, B.: Heterogeneous sulfate aerosol formation mechanisms during wintertime Chinese haze events: air quality model assessment using observations of sulfate oxygen isotopes in Beijing, Atmos Chem Phys, 19, 6107-6123, 10.5194/acp-19-6107-2019, 2019.
Shao, P., Tian, H., Sun, Y., Liu, H., Wu, B., Liu, S., Liu, X., Wu, Y., Liang, W., Wang, Y., Gao, J., Xue, Y., Bai, X., Liu, W., Lin, S., and Hu, G.: Characterizing remarkable changes of severe haze events and chemical compositions in multi-size airborne particles (PM1, PM2.5 and PM10) from January 2013 to 2016-2017 winter in Beijing, China, Atmos Environ, 189, 133-144, 10.1016/j.atmosenv.2018.06.038, 2018.
Shen, X. J., Sun, J. Y., Zhang, Y. M., Wehner, B., Nowak, A., Tuch, T., Zhang, X. C., Wang, T. T., Zhou, H. G., Zhang, X. L., Dong, F., Birmili, W., and Wiedensohler, A.: First long-term study of particle number size distributions and new particle formation events of regional aerosol in the North China Plain, Atmos Chem Phys, 11, 1565-1580, 10.5194/acp-11-1565-2011, 2011.
Song, S., Gao, M., Xu, W., Sun, Y., Worsnop, D. R., Jayne, J. T., Zhang, Y., Zhu, L., Li, M., Zhou, Z., Cheng, C., Lv, Y., Wang, Y., Peng, W., Xu, X., Lin, N., Wang, Y., Wang, S., Munger, J. W., Jacob, D. J., and McElroy, M. B.: Possible heterogeneous chemistry of hydroxymethanesulfonate (HMS) in northern China winter haze, Atmos Chem Phys, 19, 1357-1371, 10.5194/acp-19-1357-2019, 2019a.
Song, S., Nenes, A., Gao, M., Zhang, Y., Liu, P., Shao, J., Ye, D., Xu, W., Lei, L., Sun, Y., Liu, B., Wang, S., and McElroy, M. B.: Thermodynamic Modeling Suggests Declines in Water Uptake and Acidity of Inorganic Aerosols in Beijing Winter Haze Events during 2014/2015-2018/2019, Environ Sci Tech Let, 6, 752-760, 10.1021/acs.estlett.9b00621, 2019b.
Wang, G., Zhang, R., Gomez, M. E., Yang, L., Zamora, M. L., Hu, M., Lin, Y., Peng, J., Guo, S., and Meng, J.: Persistent sulfate formation from London Fog to Chinese haze, Proceedings of the National Academy of Sciences, 113, 13630-13635, 2016.
Wang, J., Zhao, B., Wang, S., Yang, F., Xing, J., Morawska, L., Ding, A., Kulmala, M., Kerminen, V.-M., Kujansuu, J., Wang, Z., Ding, D., Zhang, X., Wang, H., Tian, M., Petaja, T., Jiang, J., and Hao, J.: Particulate matter pollution over China and the effects of control policies, Sci Total Environ, 584, 426-447, 10.1016/j.scitotenv.2017.01.027, 2017.
Wang, S., Xing, J., Jang, C., Zhu, Y., Fu, J. S., and Hao, J.: Impact Assessment of Ammonia Emissions on Inorganic Aerosols in East China Using Response Surface Modeling Technique, Environ Sci Technol, 45, 9293-9300, 10.1021/es2022347, 2011a.
Wang, X., Wei, W., Cheng, S., Zhang, C., and Duan, W.: A monitoring-modeling approach to SO42- and NO3- secondary conversion ratio estimation during haze periods in Beijing, China, Journal of environmental sciences (China), 78, 293-302, 10.1016/j.jes.2018.11.002, 2019.
Wang, Z. B., Hu, M., Yue, D. L., Zheng, J., Zhang, R. Y., Wiedensohler, A., Wu, Z. J., Nieminen, T., and Boy, M.: Evaluation on the role of sulfuric acid in the mechanisms of new particle formation for Beijing case, Atmos Chem Phys, 11, 12663-12671, 10.5194/acp-11-12663-2011, 2011b.
Wang, Z. B., Hu, M., Mogensen, D., Yue, D. L., Zheng, J., Zhang, R. Y., Liu, Y., Yuan, B., Li, X., Shao, M., Zhou, L., Wu, Z. J., Wiedensohler, A., and Boy, M.: The simulations of sulfuric acid concentration and new particle formation in an urban atmosphere in China, Atmos Chem Phys, 13, 11157-11167, 10.5194/acp-13-11157-2013, 2013a.
Wang, Z. B., Hu, M., Sun, J. Y., Wu, Z. J., Yue, D. L., Shen, X. J., Zhang, Y. M., Pei, X. Y., Cheng, Y. F., and Wiedensohler, A.:

Characteristics of regional new particle formation in urban and regional background environments in the North China Plain, Atmos Chem Phys, 13, 12495-12506, 10.5194/acp-13-12495-2013, 2013b.
Weber, R., McMurry, P. H., Mauldin, R., Tanner, D., Eisele, F., Clarke, A., and Kapustin, V.: New particle formation in the remote troposphere: A comparison of observations at various sites, Geophys Res Lett, 26, 307-310, 1999.
Wu, Z., Hu, M., Liu, S., Wehner, B., Bauer, S., Ma ßling, A., Wiedensohler, A., Petäjä, T., Dal Maso, M., and Kulmala, M.: New particle formation in Beijing, China: Statistical analysis of a 1-year data set, J Geophys Res, 112, 10.1029/2006jd007406, 2007.
Xia, Y., Zhao, Y., and Nielsen, C. P.: Benefits of China's efforts in gaseous pollutant control indicated by the bottom-up emissions and satellite observations 2000–2014, Atmos Environ, 136, 43-53, 2016.
Yue, D., Hu, M., Wu, Z., Wang, Z., Guo, S., Wehner, B., Nowak, A., Achtert, P., Wiedensohler, A., Jung, J., Kim, Y. J., and Liu, S.: Characteristics of aerosol size distributions and new particle formation in the summer in Beijing, J Geophys Res-Atmos, 114, 10.1029/2008jd010894, 2009.
Zeng, Y., Cao, Y., Qiao, X., Seyler, B. C., and Tang, Y.: Air pollution reduction in China: Recent success but great challenge for the future, Sci Total Environ, 663, 329-337, 10.1016/j.scitotenv.2019.01.262, 2019.
Zhai, S., Jacob, D. J., Wang, X., Shen, L., Li, K., Zhang, Y., Gui, K., Zhao, T., and Liao, H.: Fine particulate matter (PM2.5) trends in China, 2013-2018: separating contributions from anthropogenic emissions and meteorology, Atmos Chem Phys, 19, 11031-11041, 10.5194/acp-19-11031-2019, 2019.
Zhang, R., Khalizov, A., Wang, L., Hu, M., and Xu, W.: Nucleation and growth of nanoparticles in the atmosphere, Chem Rev, 112, 1957-2011, 10.1021/cr2001756, 2012.
Zhang, R., Wang, G., Guo, S., Zarnora, M. L., Ying, Q., Lin, Y., Wang, W., Hu, M., and Wang, Y.: Formation of Urban Fine Particulate Matter, Chemical Reviews, 115, 3803-3855, 10.1021/acs.chemrev.5b00067, 2015.
Zhang, S., Xing, J., Sarwar, G., Ge, Y., He, H., Duan, F., Zhao, Y., He, K., Zhu, L., and Chu, B.: Parameterization of heterogeneous reaction of SO2 to sulfate on dust with coexistence of NH3 and NO2 under different humidity conditions, Atmos Environ, 208, 133-140, 10.1016/j.annosenv.2019.04.004, 2019.
Zhao, B., Wu, W., Wang, S., Xing, J., Chang, X., Liou, K.-N., Jiang, J. H., Gu, Y., Jang, C., Fu, J. S., Zhu, Y., Wang, J., Lin, Y., and Hao, J.: A modeling study of the nonlinear response of fine particles to air pollutant emissions in the Beijing-Tianjin-Hebei region, Atmos Chem Phys, 17, 12031-12050, 10.5194/acp-17-12031-2017, 2017.
Zhao, B., Zheng, H., Wang, S., Smith, K. R., Lu, X., Aunan, K., Gu, Y., Wang, Y., Ding, D., Xing, J., Fu, X., Yang, X., Liou, K.-N., and Hao, J.: Change in household fuels dominates the decrease in PM2.5 exposure and premature mortality in China in 2005-2015, P Natl Acad Sci USA, 115, 12401-12406, 10.1073/pnas.1812955115, 2018.
Zheng, B., Tong, D., Li, M., Liu, F., Hong, C., Geng, G., Li, H., Li, X., Peng, L., Qi, J., Yan, L., Zhang, Y., Zhao, H., Zheng, Y., He, K., and Zhang, Q.: Trends in China's anthropogenic emissions since 2010 as the consequence of clean air actions, Atmos. Chem. Phys., 18, 14095-14111, 10.5194/acp-18-14095-2018, 2018.
Zheng, G., Duan, F., Ma, Y., Zhang, Q., Huang, T., Kimoto, T., Cheng, Y., Su, H., and He, K.: Episode-Based Evolution Pattern Analysis of Haze Pollution: Method Development and Results from Beijing, China, Environ Sci Technol, 50, 4632-4641, 10.1021/acs.est.5b05593, 2016.
Zheng, G. J., Duan, F. K., Su, H., Ma, Y. L., Cheng, Y., Zheng, B., Zhang, Q., Huang, T., Kimoto, T., Chang, D., Poeschl, U., Cheng, Y. F., and He, K. B.: Exploring the severe winter haze in Beijing: the impact of synoptic weather, regional transport and heterogeneous reactions, Atmos Chem Phys, 15, 2969-2983, 10.5194/acp-15-2969-2015, 2015a.
Zheng, H., Zhao, B., Wang, S., Wang, T., Ding, D., Chang, X., Liu, K., Xing, J., Dong, Z., Aunan, K., Liu, T., Wu, X., Zhang, S., and Wu, Y.: Transition in source contributions of PM2.5 exposure and associated premature mortality in China during 2005-2015, Environ Int, 132, 10.1016/j.envint.2019.105111, 2019.
Zheng, J., Khalizov, A., Wang, L., and Zhang, R.: Atmospheric Pressure-Ion Drift Chemical Ionization Mass Spectrometry for Detection of Trace Gas Species, Anal Chem, 82, 7302-7308, 10.1021/ac101253n, 2010.
Zheng, J., Hu, M., Zhang, R., Yue, D., Wang, Z., Guo, S., Li, X., Bohn, B., Shao, M., He, L., Huang, X., Wiedensohler, A., and Zhu, T.: Measurements of gaseous H2SO4 by AP-ID-CIMS during CAREBeijing 2008 Campaign, Atmos Chem Phys, 11, 7755-7765, 10.5194/acp-11-7755-2011, 2011.

569 Zheng, J., Yang, D., Ma, Y., Chen, M., Cheng, J., Li, S., and Wang, M.: Development of a new corona discharge based ion
570 source for high resolution time-of-flight chemical ionization mass spectrometer to measure gaseous H2SO4 and aerosol sulfate,
571 Atmos Environ, 119, 167-173, 10.1016/j.atmosenv.2015.08.028, 2015b.

572